PHYSICAL REVIEW B VOLUME 17, NUMBER 7 1 APRIL 1978

Transmission-electron spin resonance in dilute CuFe alloys

A. L. Ritter
Virginia Polytechnic Institute and State University, Blacksburg, Virginia 24061

R. H. Silsbee
Laboratory of Atomic and Solid State Physics and Materials Science Center, Cornell University, Ithaca, New York 14853

(Received 31 May 1977)

Alloys of Cu with nominally 5- and 10-at. ppm Fe were studied by transmission-electron spin resonance (TESR) in the temperature range 2–40 K. The samples were strained in order to remove background signals which hamper analysis of TESR in relatively pure metal films. These measurements represent the first reported observation of electron spin resonance in a dilute magnetic alloy below its Kondo temperature. The relaxation rate of these alloys roughly scales with Fe concentration and exhibits a clear minimum at approximately 25 K. The contribution of the Fe impurities to the relaxation rate of the alloys is $(7.7 \pm 0.9) \times 10^8$/sec. at. ppm at 25K. The g value of the alloys did not deviate from the g value of pure Cu within the experimental scatter. We analyze our results in terms of coupled Bloch equations and discuss possible mechanisms for the inferred local-moment–lattice and conduction-electron–lattice relaxation rates.

I. INTRODUCTION

We report a study of very dilute Fe impurities in Cu using transmission-electron spin resonance (TESR). This traditional "Kondo" system exhibits many intriguing physical properties arising from the dynamic interaction between the local Fe moment and the conduction-electron spins. It has long been recognized that electron-spin resonance would be a sensitive probe of the coupled spin system in the interesting temperature regime below T_K which is approximately 20 K for CuFe, but experimental difficulties have precluded measurements on this particular system. Our measurements which were taken from 2 to 40 K are the first reported observations of electron-spin resonance in a Kondo system at temperatures of the order of and less than the characteristic Kondo temperature. The concentration of Fe in our samples is sufficiently low ($5 \rightarrow 10$ ppm) that impurity-impurity interactions can reasonably be ignored, thus allowing us to observe the single-impurity effects which are of interest.

We have analyzed our results in terms of phenomenological Bloch equations of the form first suggested by Hasegawa.[1] Experiments on dilute Mn and Cr impurities in Cu and Ag hosts[2,3] have been interpreted in terms of these coupled equations and are reasonably consistent with the "bottleneck" limit of this model. The model has been placed on a firmer theoretical basis for temperatures above T_K by subsequent work,[4–9] but neither theoretical insight nor experimental evidence exists for the dynamic behavior of strongly coupled spin systems below the Kondo temperature. In the absence of a theory for spin systems in this temperature regime, we have used the coupled Bloch equations as a framework for discussion of our results.

In order to describe the behavior of Mn and Cr impurities in noble-metal hosts by this model, it was necessary to invoke a phenomenological local-moment–lattice relaxation ω_{dl} whose physical basis is still not understood. A second purpose of our study was to throw light on this relaxation mechanism. Some suggested origins of ω_{dl} have appeared in the literature; in particular, Sweer *et al.*[5] have suggested two general forms for ω_{dl} which they call static and dynamic processes. These two mechanisms do not appear to have the correct temperature dependence to explain the data for Mn and Cr in Cu, but in our case the temperature dependence of ω_{dl} for CuFe conceivably can be explained by the static mechanism. We discuss the possibility it also may be consistent with the dynamic process.

A fundamental question which is of interest in the dilute-impurity problem is the structure of the magnetic ion when it is in a simple-metal host. Several models exist for the impurity which can be divided roughly into two categories; the spin-fluctuation model which is a phenomenological extension of the Friedel-Anderson model and various versions of the ionic model. There are three variations of the ionic model which may describe Fe in Cu. They each make

qualitative and in some cases quantitative predictions for the magnitude of ω_{dl} if it arises from either the static or dynamic process suggested by Sweer *et al.* Unfortunately, the unknown effect of the Kondo interaction prevents us from conclusively favoring one version over another. The spin-fluctuation model makes fewer explicit predictions to compare with our experiment, but some qualitative features of this model have been discussed.

A ubiquitous problem which hampers most TESR experiments on reasonably pure samples is the large field-dependent background due to cyclotron modes. These modes are effective in the transmission of power through the sample when the conduction-electron mean-free path is comparable to the sample thickness. The problem is particularly severe in the attempt to study Fe in Cu because the very large broadening of the TESR by the Fe (~60 G/ppm) implies the need to work at very low iron concentrations <10 ppm, where the electron mean-free path is still quite large. This cyclotron background has been suppressed in these experiments by cold working the foils, by rolling, which results in sufficient electron scattering by dislocations and defects to avoid the background problem without introducing a very significant increase in the TESR linewidth. The penalty imposed by this procedure is some ambiguity in the effective Fe concentration because of the possibility of interaction of the Fe with the defects introduced by the cold working of the samples.

II. THEORY

A. TESR in systems with dilute magnetic impurities

TESR is an ideal technique for studying the resonance response of the conduction-electron spins in a metal. When the conduction-electron spins are driven at one face of a thin foil (typically 25–50 μm thick) by a microwave field which satisfies their Larmor condition, the induced transverse magnetization can diffuse across the film and be detected at the other side of the foil. A characteristic length which governs the resonance line shape and intensity is the spin depth which is the distance the spin will diffuse before suffering a spin-flip collision. When this parameter is larger than the film thickness, the transmitted signal will be the characteristic Lorentzian response of the spin system. If it is less than the film thickness, the line shape is modified in a manner which has been analyzed in detail by Dunifer.[10] Using his analysis, the effective relaxation rate and g value can be extracted from the experimental line shape.

If magnetic impurities are in the sample and couple to the conduction-electron spins, they can affect strongly the conduction-spin resonance. For example, if the impurity g value is different from that of the conduction electrons and if the spin systems are not too strongly coupled (what is meant by strongly coupled will be defined later), then the conduction-spin resonance will be shifted by an amount proportional tc the local-moment susceptibility in a manner analogous to the Knight shift (actually the converse, i.e., the "Day" shift). An additional relaxation of the conduction electrons to the local moment also will be present. On the other hand, if the coupling between the two spins systems is sufficiently strong, their response to the driving field will be characteristic of coupled modes. This is the now familiar "bottleneck" effect. In this case the effective g value is a susceptibility weighted average of the respective g values of the two systems, while the effective relaxation rate is a similar average of the impurity-moment–lattice relaxation and conduction-electron–lattice relaxation. These results and the intermediate behavior of a coupled system can be derived from Bloch equations.

B. Coupled Bloch equation

Schultz *et al.*[9] have suggested the most general form the coupled Bloch equations might take on the basis of symmetry arguments. For the case of isotropic exchange coupling between the local moment and the conduction-electron spins, these equations can be written

$$\frac{d\vec{M}_s}{dt} = \gamma_s(\vec{H}+\lambda\vec{M}_d)\times\vec{M}_s + D_0\nabla^2[M_s-\chi_s(H+\lambda M_d)] + \left(\frac{\gamma_s}{\gamma_d}\right)\omega_{ds}[M_d-\chi_d(H+\lambda M_s)] - (\omega_{sd}+\omega_{sl})[M_s-\chi_s(H+\lambda M_d)] \quad , \tag{1}$$

$$\frac{dM_d}{dt} = \gamma_d(\vec{H}+\lambda\vec{M}_s)\times\vec{M}_d + \left(\frac{\gamma_d}{\gamma_s}\right)\omega_{sd} \times[M_s-\chi_s(H+\lambda M_d)] - (\omega_{ds}+\omega_{dl})[M_d-\chi_d(H+\lambda M_s)] \quad , \tag{2}$$

where in general all parameters may be functions of frequency, magnetic field, and temperature. In a series of papers[4,5] these transport equations for the local-moment and conduction-electron magnetization have been derived rigorously from the Kondo exchange Hamiltonian to second order in the exchange-coupling strength. The perturbative derivation, of course, breaks down below the Kondo temperature. We list in Table I the various parameters which appear in Eqs. (1) and (2) and the corresponding expressions which have been derived by Sweer *et al.*[5] The meaning of static and dynamic ω_{dl} will be discussed in Sec. II C.

The various terms which appear in the coupled

equations have the following physical basis. A diffusion term for the conduction-electron magnetization has been included explicitly to account for the conduction-electron mobility which makes TESR possible. The molecular field of one system acting on the other is represented in the torque terms by $\lambda M_{s,d}$. The cross relaxation rate ω_{sd} and ω_{ds} are, respectively, the Overhauser and Korringa rate which are given in the first Born approximation in Table I. The conduction-electron–lattice relaxation ω_{sl} arises from spin-orbit scattering from impurities and phonons. Relaxation from impurity scattering is temperature independent, while relaxation to phonons goes approximately as T^4 or T^5 and is generally negligible below 25 K. The direct local-moment–lattice relaxation ω_{dl} is a phenomenological parameter whose origin is still obscure.

These coupled equations can be solved approximately in the two limits described at the beginning of this section. The weak coupling, or nonbottleneck, limit occurs when the cross relaxation rates are slower than the relaxation of the local moment and conduction electrons to the lattice. The observed TESR will have an effective gyromagnetic ratio and relaxation rate

$$\gamma_{\text{eff}} = \gamma_s(1+\lambda\chi_d) \ ,$$

$$\omega_{\text{eff}} = \omega_{sd} + \omega_{sl} \ .$$

In the opposite limit when the cross relaxation is faster than ω_{sl} and ω_{dl} [also faster than $\gamma_{s,d}\lambda M_{s,d}$ and $(\gamma_s - \gamma_d)H$], the system is bottlenecked and γ_{eff} and ω_{eff} are

$$\gamma_{\text{eff}} = \frac{\gamma_s + (\gamma_s/\gamma_d)^2\chi_r\gamma_d}{1+(\gamma_s/\gamma_d)^2\chi_r} \ ,$$

$$\omega_{\text{eff}} = \frac{\omega_{sl} + (\gamma_s/\gamma_d)^2\chi_r\omega_{dl}}{1+(\gamma_s/\gamma_d)^2\chi_r} \ ,$$

where $\chi_r = \chi_d/\chi_s$. The concept of strongly coupled modes has been well established for CuCr,[2] and CuMn.[3] The TESR data for CuCr could be fit quite well by the strong coupling Bloch equations over a range $0.01 \leq \chi_r \leq 10$. CuMn was consistent also with the bottleneck limit, but in this case some unexplained anomalies did exist.

In the CuFe systems discussed in this paper, χ_r is always much less than one because of the low-impurity concentration and the large Weiss constant appearing in the Fe susceptibility. A general solution of the coupled equations can be found in this case which is correct to order χ_r. The effective relaxation rate and gyromagnetic ratio are

TABLE I. Correspondence between the parameters of the generalized Bloch equation suggested by Schultz *et al.* (Ref. 9) and the perturbative expansions for two possible models of ω_{dl} derived by Sweer *et al.* (Ref. 5). J is the isotropic exchange coupling constant and $\rho = 1/D$ is the conduction-electron density of states. n is the density of electrons, while N is the number of impurities. γ_s and γ_{d0} are the unperturbed ($J=0$) gyromagnetic ratios for the conduction-electron and impurity spins, respectively. $\gamma_d^2\langle\omega_n^2\rangle$ is the second moment of the static-field distribution experienced by the impurity. ω_{sl}^0 is the conduction-electron–lattice relaxation rate when $J=0$.

Parameter	Perturbative expression	
	Dynamic ω_{dl}	Static ω_{dl}
$\lambda = \alpha_1$	$J/\gamma_s\gamma_{d0}n$	Same
α_2	$(J/n)^2(\rho/\gamma_s\gamma_{d0})\ln(k_BT/D)$	Same
γ_d	$\gamma_{d0}[1+\alpha_2\chi_s(1-\gamma_s/\gamma_{d0}+\omega_{dl}/\omega_{ds})]$	$\gamma_{d0}[1+\alpha_2\chi_s(1-\gamma_s/\gamma_{d0})]$
χ_s	$\frac{1}{2}\rho(\hbar\gamma_s)^2$	Same
χ_d	$\frac{NS(S+1)(\hbar\gamma_{d0})^2}{3k_BT[1+[\alpha_1-2\alpha_2(1+\omega_{dl}/\omega_{ds})]\chi_s]}$	$\frac{NS(S+1)(\hbar\gamma_{d0})^2}{3k_BT[1+(\alpha_1-2\alpha_2)\chi_s]}$
ω_{sd}	$\frac{2\pi}{3\hbar}\left[\frac{J}{n}\right]^2\rho NS(S+1)$	Same
ω_{ds}	$\frac{\pi}{\hbar}\left[\frac{J}{n}\right]^2\rho^2k_BT$	Same
ω_{dl}	ω_{dl}	$\frac{\langle\omega_n^2\rangle(1-\alpha_2\chi_s)^{-1}}{\omega_{ds}-i[\omega-\gamma_dH[1+(\alpha_1+\alpha_2)\chi_s]]}$
ω_{sl}	$\omega_{sl}^0 - 3\alpha_2\chi_s(\omega_{sd}/\omega_{ds})\omega_{dl}$	$\omega_{sl}^0 - \alpha_2\chi_s(\omega_{sd}/\omega_{ds})\omega_{dl}$

$$\gamma_{\text{eff}} = \gamma_s + \left(\frac{\gamma_d - \gamma_s}{1 + \frac{\omega_{dl}}{\omega_{ds}}}\right)\left(\frac{\gamma_s}{\gamma_d}\right)^2 \chi_r + \frac{\gamma_s \lambda \chi_d \left(\frac{\omega_{dl}}{\omega_{ds}}\right)}{\left(1 + \frac{\omega_{dl}}{\omega_{ds}}\right)^2}\left(1 + \frac{\omega_{dl}}{\omega_{ds}} - \frac{\gamma_s}{\gamma_d}\right), \quad (3)$$

$$\omega_{\text{eff}} = \omega_{sl} + \left(\frac{\omega_{dl} - \omega_{sl}}{1 + \frac{\omega_{dl}}{\omega_{ds}}}\right)\left(\frac{\gamma_s}{\gamma_d}\right)^2 \chi_r , \quad (4)$$

where it has been assumed that the cross relaxation rates are larger than both the molecular-field terms and the difference in the Larmor frequency of the impurity and conduction-electron spins. These conditions are thought to be satisfied in the CuFe system. It should be noted that in the limit ω_{dl}/ω_{ds} large (small) these expressions go properly to the appropriate nonbottleneck (bottleneck) limit (detailed balance implies $\gamma_s^2 \chi_d \omega_{ds} = \gamma_d^2 \chi_s \omega_{sd}$).

C. Direct local-moment–lattice relaxation

The primary difficulty in explaining the dynamic behavior of coupled-spin systems in terms of the coupled Bloch equations has been to understand the origin and physical basis for ω_{dl}. Studies on CuMn,[3] and CuCr[2] which included data well above T_K so that complications due to the Kondo effect should have been minimal, revealed respective relaxation rates of approximately 2.6×10^8/sec and 2.2×10^9/sec which seemed to be independent of temperature. The lack of temperature dependence has been the most difficult feature to understand. It immediately rules out phonon processes which, in general, are also too weak. There are two general forms of ω_{dl} suggested by Sweer *et al.*[5] in their modeling of the coupled-mode problem.

The first form they considered was a real relaxation process which was modeled by assuming the local-moment couples to a fictitious set of conduction-electron spins to which it can relax by mutual spin flip. It is assumed further that this fictitious bath always remains in equilibrium, so that it does not bottleneck like the real conduction-electron spin system. The authors suggested that the process considered by Yafet[11] might be an example of this mechanism. Another example is some interaction which couples the local moment to the conduction-electron orbital degrees of freedom, an idea suggested by Hirst.[12] Both these examples are Korringa-like relaxation processes and hence, are proportional to temperature and do not match the temperature independent ω_{dl} deduced for CuMn,[3] and CuCr.[2] A second general source which might simulate ω_{dl} is a static broadening arising possibly from the hyperfine interaction, frozen in fields due to impurity-impurity interaction, or inhomogeneous width from strain effects. In general the resonance line shape in the presence of these effects is a complicated function of resonance frequency, temperature, and exchange-coupling strength; it has been considered in detail by several authors.[13–15] In the strong-coupling limit, i.e., when the local moment relaxation rate ω_{ds} is greater than the inhomogeneous width ΔH, one expects on the basis of motional narrowing arguments that ω_{dl} will be proportional to $(\Delta H)^2/\omega_{ds}$ and hence inversely proportional to temperature, again in disaccord with experiments.[2,3]

D. Models of the impurity state

The nature of the coupling between the impurity and conduction-electron spins and possible mechanisms for ω_{dl} both depend sensitively on the model chosen to describe the impurity. For example, if the impurity is viewed as having only a spin degree of freedom which couples to the conduction-electron spins via isotropic exchange, it is very difficult to conceive of an ω_{dl} process. When the orbital degrees of freedom of the impurity are considered, then possible mechanisms for ω_{dl} can be imagined which have the correct magnitude though all which have been suggested so far, still appear to have the wrong temperature dependence. In order to explore the question of the proper model for Fe in Cu, we have analyzed our results in terms of the four models listed in Table II which are thought to be applicable to this system.

These models can be divided into two general categories: ionic models and the spin-fluctuation model. The ionic model has been discussed in detail by Hirst.[12,16–18] It assumes the impurity is in a unique configuration of n electrons. The mixing interaction between the local orbitals and extended conduction-band states couples the ground state to configurations of $n \pm 1$ electrons and gives in second order an effective exchange interaction. The spin-fluctuation model,[19] on the other hand, assumes the spin and orbital moment fluctuate independently with characteristic rates $1/\tau_{\text{spin}}$ and $1/\tau_{\text{orb}}$, respectively. It is assumed that in CuFe the relation

$$1/\tau_{\text{spin}} < k_B T/\hbar < 1/\tau_{\text{orb}}$$

is satisfied above the Kondo temperature, so that the impurity appears to have a spin moment but not an orbital moment. The magnetic properties of the impurity are determined primarily by the spin moment with the orbital fluctuations contributing a temperature-independent term to the total susceptibility.

TABLE II. Models of dilute Fe impurities in a Cu host. V is the crystal-field potential at the impurity site arising from crystal strain. Δ is the cubic crystal-field splitting. The theoretical ratio ω_{dl}/ω_{ds} for the three ionic models is from Hirst (Ref. 12). The experimental ratio is based on the model predictions of the impurity g value.

Model	Atomic configuration	Crystal field	Spin-orbit multiplet	g value	Sensitivity to strain	ω_{dl}/ω_{ds} Theor.	Expt.
Ionic							
$Fe^{++}(3d^6)$	^5D	$^5T_2$	$J=1$	$\frac{7}{2}$	V	1.15	0.12 ± 0.05
$Fe^{+}(3d^7)$	^4F	$^4T_1$	$J=\frac{1}{2}$	$\frac{13}{3}$	0	0.08	0.20 ± 0.09
$Fe^{+}(3d^7)$	^4F	$^4A_2$	$J=\frac{3}{2}$	2	V^2/Δ	0	0.037 ± 0.015
Spin fluctuation	$S=\frac{3}{2}$			2	weak?	?	0.037 ± 0.015

Since the ground-state configuration of Fe in Cu has not been clearly established, there exist three possible variations of the ionic model which might reasonably describe this system. Hirst assumed that Fe would be in the divalent configuration in metal hosts,[18] but in view of the instability between the monovalent and divalent configuration across the transition-metal series, it does not seem reasonable to rule out the monovalent configuration yet. The Hund's rule ground state for each ionic model is given in the first column of Table II. The degeneracy of this state is successively reduced by the crystal-field potential and spin-orbit interaction. The respective lowest-lying states are given in the next two columns. The first two models assume the normal sign of the crystal field (positive point charge neighbors), while the third assumes an inverted sign. In the next column is listed the impurity g value predicted by the model. The next column gives the predicted dependence of the impurity resonance on strain energy. It will be discussed in Sec. IV C in connection with the static mechanism for ω_{dl}. The last two columns are the theoretical and experimental ratios of ω_{dl} and ω_{ds}. The theoretical ratio was calculated by Hirst[12] for the three ionic models and will be discussed in Sec. IV C.

III. EXPERIMENT

A. Sample preparation

Our samples were prepared by standard dilution techniques. The starting material for the master alloy was 99.9%-pure Fe from Glidden Metals, Inc. and 99.999%-pure Cu from Cominco, Inc. The constituent materials for the master alloys were melted together in graphite crucibles using a vacuum induction furnace. The alloy was homogenized in the melt for 10 min, then quenched in a chilled copper mold. A 100-at. ppm master alloy was prepared in this manner by two dilutions and its homogeneity was checked by atomic absorption analysis. The concentration of Fe in different parts of the ingot agreed to within 10%.

The final samples which had nominal concentrations of 5, 10, and 15-at. ppm Fe were prepared by diluting the master alloy with a batch of Cominco copper whose total impurity content was less than 1 ppm by the company's analysis. The residual resistivity ratio [RRR $=\rho(4.2\text{ K})/\rho(273\text{ K})$] of the pure material varied between 500 and 1000 after annealing in a hydrogen atmosphere (RRR could be improved by factors of 2 or 3 by annealing in a "vacuum" of 10^{-6} to 10^{-5} Torr. Apparently residual impurities became oxidized by this anneal). The final alloys again were homogenized for 10 min in the induction furnace and quenched in a chilled copper mold. The crucibles for containing the molten metal were made of high-purity graphite which had been fired in a chlorine atmosphere.

Sample foils approximately 0.3–0.5 mm thick were spark cut from the ingots, etched lightly in dilute nitric acid, and then rolled to approximately 0.16-mm thickness. The rollers were cleaned carefully with a mild abrasive and acetone before reducing each sample. In order to check whether pressing the samples introduced a significant concentration of impurities, several pure Cu foils were prepared in parallel with our CuFe samples by the same technique. After the samples and pure copper foils were rolled, they were etched lightly and then annealed for one hour at 1000 °C under flowing dry hydrogen. The foils were not quenched after the anneal.

The inverse resistivity ratio is shown in Fig. 1 as a function of nominal impurity concentration. It has been corrected for size effects.[20] Also shown are measurements on several pure Cu foils which were prepared in the same manner as the alloys. The solid line through our data corresponds to $d\rho/dc = 7.8$ $\mu\Omega$ cm/(at. % Fe) which is somewhat lower than found in other work[21–23] where it ranges from 11 to 14 $\mu\Omega$ cm/(at. % Fe), suggesting that the real concentration of Fe in our samples may be

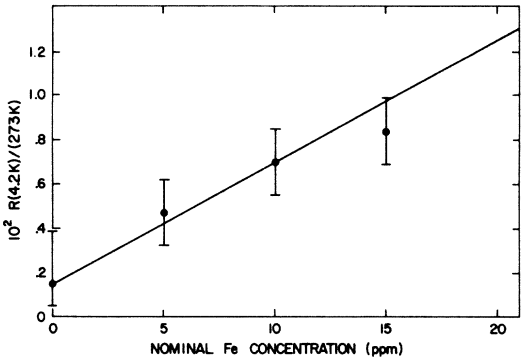

FIG. 1. Inverse resistivity ratio of CuFe alloys as a function of nominal impurity concentration.

55%–70% of the nominal value. The samples were stored in liquid nitrogen and with this precaution we found that the RRR did not change over a period of several months.

In preparation for TESR measurements, the foil was reduced in thickness typically by a factor of 2 in order to eliminate the "cyclotron background." After completing TESR measurements, the samples were etched lightly in nitric acid and reannealed in hydrogen. Then, their RRR was measured again. The error bars in Fig. 1 show the maximum dispersion of the inverse-RRR measurements before and after straining the samples. The data indicate that a significant concentration of additional impurities was not introduced when the samples were strained.

B. Spectrometer and thermometry

A conventional X-band superheterodyne transmission spectrometer was used in this experiment. Details about the spectrometer can be found in Ref. 24.

The temperature of the sample was measured by a Cryo Cal germanium resistor. Since approximately 0.1 w of microwave power is dissipated in the sample under normal operating conditions, great care was taken in the design of the cavity to insure that a significant thermal gradient did not exist between the Ge thermometer and the sample foil. The foil is thermally anchored to the cavities by two single-crystal sapphire disks which are attached to each side of the foil and to the cavity walls by N grease. The cavities in turn are coupled to the liquid-He bath by He exchange gas. The Ge thermometer is mounted in the cavity wall within a few mm of the edge of the sample foil. The maximum temperature difference which might exist between the center of the sample foil and the thermometer is estimated to be 1 K.

C. Results

The open circles in Fig. 2 show the relaxation rate of "pure Cu" as a function of temperature. This sample, prepared by the same procedures used in making the CuFe alloys, had an RRR of 600 after being annealed in hydrogen and an RRR of 67 after being strained. The relaxation rate increases rapidly above 25 K due to spin-phonon scattering while at lower temperatures the rate is expected to be constant if no magnetic impurities are present. The small upturn in the rate at low temperature we attribute to residual magnetic impurities, probably Fe. We found that unstrained Cu samples which had been annealed in a partial pressure of oxygen exhibited a temperature independent rate of $(1.7 \pm 0.2) \times 10^8$/sec below 20 K. The relaxation rate of our "pure-Cu" sample, then, has at least three contributions: a residual rate of 1.7×10^8/sec; relaxation from strains, defects, and dislocations; and finally relaxation due to residual magnetic impurities. Beuneu *et al.*[25] made a systematic study of the contribution of strains and dislocations to conduction electron spin relaxation in Cu, Ag, and Al. In all three systems, they found the additional spin-flip rate due to rolling the sample was proportional to the residual resistivity of the sample. The proportionality constant for strained Cu samples was $\Delta(1/T_2)/\Delta\rho = 9.2 \times 10^9/\text{sec}\,\mu\Omega\,\text{cm}$. The sum of the residual relaxation rate of unstrained, oxygen annealed Cu and the rate due to scattering from strains and dislocations calculated from the results of Beuneu *et al.* is indicated by a dashed line in Fig. 2. It equals 0.39×10^9/sec. The additional rate above the dashed

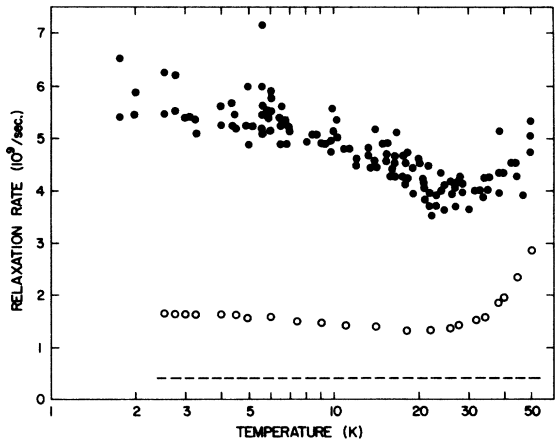

FIG. 2. Open circles are the relaxation rate as a function of temperature of strained Cu. Closed circles are the relaxation rate of 5-at. ppm CuFe alloy. The dashed line represents the contribution to the Cu and CuFe relaxation rate of the residual width observed in the best available copper samples and the width contributed by the strains induced by rolling as calculated from the RRR and Ref. 25.

line we attribute to residual Fe impurities. Scaling this additional rate with that found for our 5-ppm CuFe sample, we estimate that the concentration of Fe was of order 1 ppm, which is higher than the claimed purity of the starting material but not unreasonably so considering our subsequent treatment of it.

The g value for the pure Cu samples is temperature independent and equals 2.033 ± 0.001 in agreement with Schultz and Latham.[26]

Also shown in Fig. 2 is the effective relaxation rate for one CuFe sample whose nominal concentration is 5 at. ppm. There is now a clear minimum in the effective relaxation at approximately 25 K with the rate increasing by about 40% to an apparent plateau at the lowest temperature. Above the minimum the rate again increases rapidly due to phonon relaxation. The spin depth for this sample was a factor of 3 or 4 times less than the sample thickness which considerably reduced the signal to noise ratio and made the extraction of the effective relaxation rate quite sensitive to the resonance line shape. The primary source of scatter in our data was uncertainties in the line-shape analysis.

The effective g value of this 5-at. ppm sample as a function of temperature is shown in Fig. 3. Representative error bars are shown also. The data imply that there is no deviation of the observed g value from that of pure Cu to within the experimental uncertainty.

In Fig. 4 we show the effective relaxation rate versus temperature of two samples which contain nominally 10-at. ppm Fe. The rate has been normalized to the nominal concentration and the solid line represents the data of the 5-at. ppm sample. The signal-to-noise ratio was very poor for these samples because of the extremely broad resonance. We can conclude only that the relaxation rate roughly scales with concentration.

In order to extract the effective relaxation rate per impurity atom from our data, the real Fe concentration in the samples must be known. As discussed in

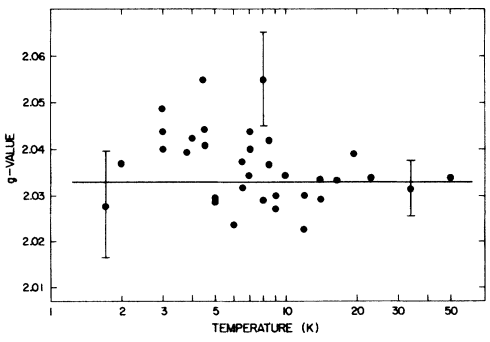

FIG. 3. Effective g value of 5-at. ppm CuFe alloy as a function of temperature.

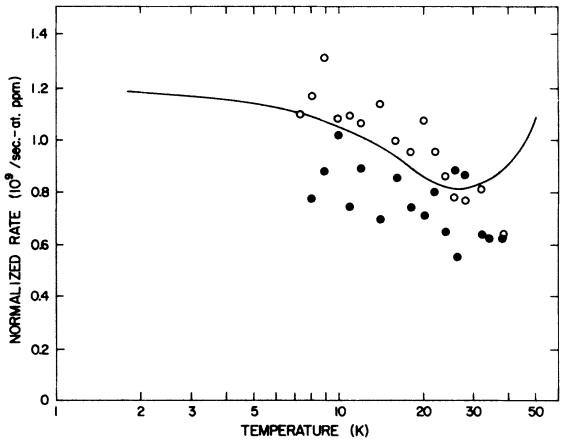

FIG. 4. Open and closed circles are the normalized relaxation rate of two CuFe alloys containing nominally 10-at. ppm CuFe. Solid line represents data for the 5-at. ppm CuFe alloy.

the introduction, some uncertainty in the effective concentration is introduced by the process of straining the sample, and our resistivity data suggest that the real concentration may be a 30%–45% smaller than the nominal concentration. Unfortunately, standard techniques of impurity analysis, such as atomic absorption and neutron activation, do not have sufficient sensitivity for Fe concentrations of a few ppm. Nor can these techniques distinguish isolated Fe impurities from clusters of impurities or from oxidized Fe atoms. An ideal technique for determining experimentally the real impurity concentration is to measure the susceptibility of the sample and separate the isolated impurity contribution from the total susceptibility. Again, in our case the low impurity concentration and weak temperature dependence of the isolated impurity susceptibility frustrate this approach. The data analysis below is in terms of the nominal concentration.

The effective relaxation rate normalized to the nominal Fe concentration can be determined from our data if it is assumed that the rates from other sources are additive, the spin-flip analog of Matthiessen's rule, and that the effective rate is linear in the nomimal concentration. We find on the basis of these assumptions that the rate at 2 K due to the Fe impurities is

$$(1.15 \pm 0.20) \times 10^9/\text{sec at. ppm} ,$$

while at 25 K the rate is

$$(7.7 \pm 0.9) \times 10^8/\text{sec at. ppm} ,$$

where the errors in these values do not reflect the systematic uncertainty in impurity concentration. The effective g-value of our 5-ppm sample did not deviate within the experimental uncertainty of ± 0.01 from the pure Cu g value.

IV. DISCUSSION

The discussion section has the following format. First, our results are analyzed in terms of Eq. (4) which is the solution of the generalized Bloch equation when χ_r is much less than one. Then a simple relation predicted by Yafet[27] between the spin-flip cross section and the orbital susceptibility of an impurity is discussed. Next, limits are placed on ω_{dl} and the extent to which CuFe is bottlenecked is determined. Finally, the origin of ω_{dl} is discussed in terms of the static and dynamic mechanisms suggested by Sweer *et al.*[5] The predicted magnitude of ω_{dl} is sensitive to the model chosen to describe the magnetic structure of the impurity. The relative merits of the four models introduced in Sec. II D are assessed on the basis of this dependence.

A. Extraction of model parameters from the Bloch equations

The relaxation rate for the 5-at. ppm sample is plotted in Fig. 5 as a function of χ_r in order to determine the parameters in Eq. (4). We take $\chi_r = 1.1/(T+27.6)$ using the analysis of Steiner *et al.*[28] for the Fe susceptibility and assuming the free-electron value for the conduction-electron susceptibility. A reasonably linear dependence between ω_{eff} and χ_r exists above $\chi_r = 2\times10^{-2}$. The upturn in ω_{eff} at higher temperature is due to phonon relaxation. Our data are consistent with ω_{dl} and ω_{sl} being independent of temperature below 25 K, but with the limited range of χ_r and our experimental scatter, it is certainly possible that both quantities may have a weak temperature dependence. Assuming they are temperature independent, our estimated linear fit to the data of Fig. 5 above $\chi_r = 2\times10^{-2}$ gives

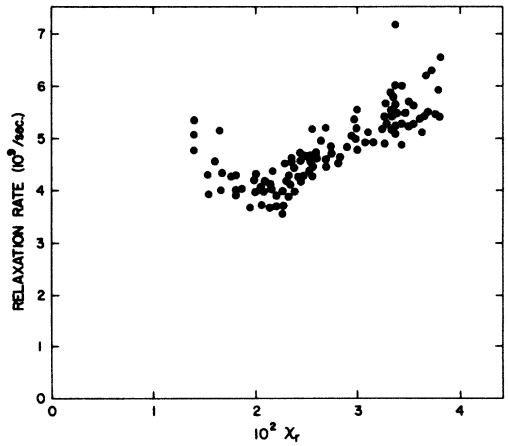

FIG. 5. Relaxation rate of 5-at. ppm CuFe alloy as a function of χ_r, the ratio of impurity to conduction-electron susceptibility [$\chi_r = 1.1/(T+27.6\text{K})$].

$$\omega_{sl} = (1.6\pm0.9)\times10^{9}/\text{sec}\ ,$$

$$\frac{(\omega_{dl}-\omega_{sl})(\gamma_s/\gamma_d)^2}{1+\omega_{dl}/\omega_{ds}} = (1.0\pm0.3)\times10^{11}/\text{sec}\ ,$$

where it is assumed that the $\chi_r = 0$ intercept is greater than 8.0×10^{8}/sec.

B. Analysis of ω_{sl}

The spin-lattice relaxation rate of our 5-ppm sample, normalized to the nominal concentration, is

$$\Delta\omega_{sl}/\Delta c = (2.4\pm1.4)\times10^{8}/\text{sec ppm}\ .$$

Monod[29] finds

$$\Delta\omega_{sl}/\Delta c = 3.9\times10^{8}/\text{sec ppm}$$

in reasonable agreement with our value considering the uncertainty in impurity concentration.

We do not know of any calculation of ω_{sl} from an ionic model. If CuFe is described by the spin-fluctuation model and has a temperature-independent orbital susceptibility, then $\Delta\omega_{sl}/\Delta c$ can be related to the orbital susceptibility by Yafet's theory.[27] A temperature-independent orbital susceptibility of $1\rightarrow1.2\times10^{-7}\mu_B/g$ has been deduced from Mössbauer and bulk-susceptibility measurements[28,30,31] Yafet derived the following expression for the spin-flip cross section $\sigma \equiv (1/2N_0\nu_F)(\Delta\omega/\Delta c)$ (N_0 is the number of host atoms per unit volume and ν_F is the Fermi velocity) associated with spin-orbit scattering from a transition-metal impurity

$$\sigma = (20\pi^3/k_F^2)\{\lambda N_d/[1-(U-J)N_d]\}^2\ ,$$

where N_d is the impurity density of states at the Fermi energy per d orbital, λ is the spin-orbit energy, and $[1-(U-J)N_d]^{-1}$ is the Hartree-Fock orbital enhancement factor. On the basis of the same model, the orbital susceptibility is

$$\chi_{\text{orb}} = 20\mu_B^2 N_d/[1-(U-J)N_d]\ .$$

Comparison of these two expressions indicates that the scattering cross section depends only on the orbital susceptibility and λ. Taking $\lambda = 426\ \text{cm}^{-1}$ from Blume and Watson[32] and $\chi = 1.0\times10^{-7}\mu_B/g$, we find $\Delta\omega_{sl}/\Delta c = 1.9\times10^{9}$/sec at. ppm in only order of magnitude agreement with our results. Given the considerable experimental and theoretical uncertainties, however, this unfavorable agreement does not provide a very strong basis for questioning the validity of the spin-fluctuation model.

C. Analysis of ω_{dl}

In order to determine ω_{dl}, we also must know ω_{ds} and g_d. Alloul[33] has inferred ω_{ds} for Fe in Cu from T_1 measurements on near-neighbor Cu nuclei. He

found that it was approximately 2.8×10^{12}/sec and was independent of temperature from 1 to 4 K. The temperature dependence of ω_{ds} is not known at higher temperatures, but it eventually is expected to be proportional to temperature. Therefore, we take Alloul's measurement as a minimum value of ω_{ds}.

Our measurement of the effective g value in the 5-ppm sample gives us no further information about g_d and ω_{dl} since there is no shift within experimental error of g_{eff} from the pure Cu g value. Therefore, these parameters cannot be uniquely determined. Reasonable limits on the ratio ω_{dl}/ω_{ds} can be found using the model predictions of g_d introduced in Sec. II D and Alloul's value of ω_{ds}. This ratio is listed in the last column of Table II.

In each case ω_{dl}/ω_{ds} is less than one, so that technically the system is bottlenecked though this will be difficult to demonstrate experimentally because ω_{dl} is so large. For example, one can never obtain the regime in which ω_{eff} is inversely proportional to the Fe concentration which is the classic signature of bottlenecked system. Similarly, in double doping experiments such as Mn and Fe in Cu, the Mn linewidth probably will be proportional to the Fe concentration for experimentally feasible levels of doping, and so it will appear that the Fe is not bottlenecking the system further. Possible mechanisms for this large relaxation rate are discussed next.

1. Static mechanism for ω_{dl}

The expression given in Table I for a static source of ω_{dl} was derived under the assumption that the impurities experience a distribution of local fields and that the second moment of the static field distribution $(\gamma^{-2}\langle\omega_n^2\rangle)^{1/2}$ is less than the applied field. The resulting expression for ω_{dl} depends in general on field and frequency which makes the solution of the coupled equations considerably more difficult. In our case, ω_{ds} is much larger than $\omega - \gamma_d H$ so that the field and frequency dependence is negligible and therefore, the equations can be solved straightforwardly as was done in Sec. II.

In the first Born approximation ω_{ds} is proportional to temperature, so that ω_{dl} for a static interaction becomes inversely proportional to temperature. Our data are not consistent with such a strong temperature dependence for ω_{dl}. On the other hand, Alloul's measurements indicate that ω_{ds} is temperature independent in the range 1–4 K which is well below the Kondo temperature. His results are consistent with Gotze's[34] predictions that the local-moment relaxation rate is enhanced strongly below T_K. Recently, Narath[35] measured the relaxation of the impurity nuclei in MoCo and WCo alloys near their Kondo temperatures and also observed an apparent enchancement of the local-moment relaxation. The evidence is strong, then, that ω_{ds} depends less strongly on temperature than the Korriga rate for $T \ll T_K$. In the opposite limit $T \gg T_K$, ω_{ds} apparently does become proportional to temperature as shown by Alloul's[36] NMR study of CuMn alloys. The temperature dependence in the critical transition region between these two limits is unfortunately not known. We only can speculate that if ω_{ds} does not increase by more than a factor of 2 or 2.5 from 2 to 30 K, then our data will still be consistent with the static mechanism for ω_{dl}.

The root-mean-square distribution of local fields can be estimated from our limits on ω_{dl} using the expression for static ω_{dl} given in Table I. We assume the Kondo corrections in this expression modify only ω_{ds} which then can be taken equal to the experimental value measured by Alloul. The resulting distribution of local fields is $26 < (\gamma^{-2}\langle\omega_n^2\rangle)^{1/2} < 68$ kG. It is much broader than the applied field in contradiction to one of the assumptions of Sweer *et al.*, but since ω_{ds} is still greater than the root-mean-square distribution, we expect that their first-order approximation is reasonably good.

There are several possible sources of static broadening. The hyperfine interaction can be excluded immediately since ^{54}Fe and ^{56}Fe, the 97% abundant isotopes, do not have nuclear moments. The Mössbauer measurements of Steiner *et al.*[37] on a very dilute CuFe alloy (estimated concentration was 10 ppm) suggest that frozen-in local fields due to the Ruderman-Kittel-Kasuya-Yosida (RKKY) interaction also are not a reasonable source. The data shown in Fig. 1 of their paper indicate that the zero-field Mössbauer line would have been a factor of 3 or 4 broader if there existed in that alloy a Lorentzian distribution of local fields whose width was of order 26 kG. Finally, random strains and defects can inhomogeneously broaden the impurity resonance. For example, Fe^{++} in MgO has an inhomogeneous width of a few thousand G which, it has been shown,[38] arises from strains and dislocations. As we will discuss, the Mössbauer line width is much less sensitive to strain than to variations in the local field. If ω_{dl} is due to a static interaction, then strain broadening appears to be the most probable mechanism.

It would have been desirable to measure ω_{dl} as a function of strain, but experimental constraints prevented us from doing this. Monod and Schultz[2] reported a preliminary value of ω_{dl} for single-crystal CuFe which agrees roughly with ours. Since their samples presumably were considerably less strained than ours, their results would indicate strain broadening is not the correct mechanism for ω_{dl}. However, their measurements did not extend much below 20 K because of cyclotron background, so the determination of ω_{dl} was very uncertain.[39]

It is useful to review the physics of strain broadening of Fe^{++} in MgO to provide a basis for discussing strain and defect interactions in a metal. The ground state of divalent Fe in a cubic crystal is triply degen-

erate. Strains, point defects, or dislocations in the host can reduce the local symmetry of the impurity, lift the threefold degeneracy of the ground state, and give zero-field splittings which may be considerably larger than the Zeeman splitting. The variation of these splittings from site to site produces the inhomogeneous spectrum. The extreme sensitivity of divalent Fe to host imperfections is a consequence of two factors: the presence of unquenched orbital angular momentum in the crystal-field ground state, and the absence of the Kramers degeneracy since there are an even number of d electrons.

The theory of inhomogeneous broadening has been reviewed by Stoneham[40] who showed that the resonance width of Fe^{++} in MgO is proportional to the square root of the dislocation density. In one nearly strain-free sample, a resonance width of 600 G corresponded to a dislocation density of $3 \times 10^6/cm^2$. The density of dislocations in our samples is of order $10^{11}/cm^2$. If we scale the resonance width by the square root of the dislocation density and ignore basic differences between magnetic impurities in insulator and metal hosts, then the inhomogeneous width of Fe in Cu would be approximately 100 kG. It is comparable to our estimated root-mean-square distribution and, though a very crude estimate, it indicates the possible magnitude of strain effects.

We argued that static fields, such as from RKKY oscillations, which had a distribution width of order 26 kG would have been clearly evident in the Mössbauer linewidth. Strain broadening, on the other hand, which arises from a distribution of resonance frequencies rather than local fields, primarily affects the Mössbauer linewidth by perturbing the local susceptibility. It may not be evident in Mössbauer data for the following reason. The local susceptibility is insensitive to strain at temperatures much larger than the induced splittings (10 K for splittings of order 85 kG) by Van Vleck's theorem,[41] and at temperatures comparable to the splittings, the Kondo effect has already begun to quench the temperature dependence of the susceptibility so that the effects of strain splittings would not be evident. It is difficult to quantify these arguments since a calculation of the local susceptibility near the Kondo temperature is difficult even for a simplified model of the impurity, but they do indicate that strain may not substantially affect the static susceptibility and thus, the Mössbauer linewidth will be left unperturbed.

The four models discussed in Sec. II D which presently are candidates to describe Fe in Cu differ substantially in their response to strains and defects. The first model suggests the ionic properties will be very sensitive to strain since splittings of the ground state level will be directly proportional to V, the crystal-field potential associated with deviation from cubic symmetry. The second model is completely insensitive to strain since the ground state is a Kramers doublet. The third model is weakly sensitive to strain; the dependence arises from an admixture of higher crystal-field levels by the strain field and thus, is proportional to V^2/Δ, where Δ is the cubic crystal-field splitting. This model is not consistent with the magnitude of strain broadening we have inferred from the static mechanism for ω_{dl}. Finally, it is difficult to assess the effect of crystal-field variations on the magnetic properties of an impurity within the assumptions of the spin-fluctuation model. Presumably the "spin" moment is coupled to the orbital motion of the d electrons by the spin-orbit interaction and hence will be affected by variations of the ion's orbital state. However, since the model assumes that the orbital contribution to the level splittings of the impurity ground state is small at low temperature, it is difficult to imagine variations in the orbital properties changing these splittings appreciably, again not by the magnitude implied by the static mechanism for ω_{dl}.

Though we cannot conclude that the static mechanism is the correct explanation for ω_{dl}, it is a conceivable theory for this parameter in the case of CuFe. The large magnitude of ω_{dl} is consistent with our intentional straining of the samples and the weak temperature dependence would be a natural consequence of the enhancement of ω_{ds} by the Kondo effect. On the other hand, confirmation of the tentative value of ω_{dl} quoted in Ref. 2 for unstrained samples would rule out strain broadening as an ω_{dl} mechanism, since it would indicate very little strain dependence of ω_{dl}. If ω_{dl} is due to strain broadening, it would be strong evidence for the original ionic model for CuFe proposed by Hirst.[18]

2. *Dynamic mechanism for* ω_{dl}

Two possible mechanisms are discussed in the literature for the dynamic relaxation of the Fe moment to the lattice. The first, analyzed by Yafet,[11] is relevant only to local-moment ions whose ground state is not orbitally degenerate, while the second, suggested by Hirst,[12] depends explicitly on the impurity ground state having orbital degeneracy. Each mechanism has the general property that the local-moment magnetization changes by one or more units while the conduction-electron magnetization remains constant. The local spin energy is transferred to the orbital motion of the conduction electrons, the "lattice," which implies a Korringa-like relaxation proportional to temperature.

Our analysis of ω_{eff} in Sec. IV A indicated that the temperature dependence of ω_{dl} must be weak; it cannot be reconciled with a Korringa process. The possibility exists that ω_{dl} is enhanced by the Kondo effect in a similar manner as ω_{ds}. Unfortunately, in constrast to ω_{ds}, neither a theoretical nor an experimental basis exists for this conjecture. Therefore, a complete analysis in terms of a dynamic mechanism for ω_{dl}

must wait until the influence of the Kondo effect on its temperature dependence is understood better. We will make a rudimentary analysis in terms of the models suggested by Yafet and Hirst assuming that ω_{dl} does become temperature independent in a manner similar to ω_{ds}.

Yafet actually suggested two mechanisms for ω_{dl} both of which are somewhat complicated and contain parameters which are poorly known. An order-of-magnitude estimate of these rates can be made by noting that for each mechanism

$$\omega_{dl} \propto \lambda^2 V_{kd}^4 N_d^2 kT/U^4 \ ,$$

where U is the effective intra-atomic Coulomb energy, λ is the local spin-orbit energy, V_{kd} is the coupling interaction between the local orbitals and the conduction-band states, and N_d is the impurity density of states at the Fermi surface. The direct exchange interaction can be written in terms of these same parameters

$$\omega_{ds} \propto V_{kd}^4 N_d^2 kT/U^2 \ ,$$

which implies

$$\omega_{dl}/\omega_{ds} \sim \lambda^2/U^2 \sim 10^{-4} \ .$$

It seems that this mechanism is two or three orders of magnitude too weak to explain our measured value of ω_{dl}/ω_{ds}.

The mechanism for ω_{dl} suggested by Hirst is based on the ionic model from which he derives an effective-exchange Hamiltonian which couples the local moment to both the spin and orbital degrees of freedom of the conduction electrons. The impurity moment may relax either by spin-flip scattering with the conduction electrons or by transferring its energy to their orbital motion. The determination of these two rates, ω_{ds} and ω_{dl}, is an exercise in tensor analysis which Hirst[12] has worked out in detail. His calculated ratios of ω_{dl}/ω_{ds} are listed in Table II. The ratio has not been calculated for the spin-fluctuation model.

The first ionic model predicts a value of ω_{dl}/ω_{ds} which is an order of magnitude larger than was measured. The theoretical ratio will not be reduced by strains or defects as long as the strain splittings are less than $k_B T$. The second ionic model predicts a ratio ω_{dl}/ω_{ds} that is a factor of 2 less than experiment. The experimental value, though, is quite sensitive to the choice of impurity g value. If, in this case, the impurity g value were somewhat less than $\frac{13}{3}$, the experimental and theoretical ratio would be in better agreement. The third model predicts $\omega_{dl}=0$ since the orbital ground state is nondegenerate. In this case, the relaxation mechanisms suggested by Yafet are relevant, but again they predict rates which are much too small to explain our data. The spin-fluctuation model predicts $\omega_{dl}=0$ since it is generally assumed that the spin and orbital moments fluctuate independently. If one postulates a residual coupling between the two moments through the spin-orbit interaction, then it is possible that the component of the orbital-fluctuation spectrum at the Larmor frequency of the spin moment may relax it. Calculation of this rate requires a much more detailed analysis of the spin-fluctuation model than is presently available.

D. Summary

In conclusion hard data have been presented for the effective relaxation rate of dilute CuFe alloys in the temperature region well below T_K. Our results have been analyzed in terms of coupled Bloch equations and it is found that the CuFe system is bottlenecked. A large, apparently temperature-independent relaxation of the local moment to the lattice is inferred. Present mechanisms for this relaxation process can conceivably explain our data, but we emphasize again that they do not seem consistent with the temperature independence of ω_{dl} in CuCr and CuMn alloys. It is clear that a more comprehensive theory of this relaxation mechanism is still desperately needed.

ACKNOWLEDGMENTS

This work has been supported by the U.S. ERDA under Contract No. AT(11-1)-3150, Technical Report No.C00-3150-39 and the NSF under Grant No. DMR-74-20689. Additional support was received from the NSF under Grant No. DMR-76-01281 through the Cornell Materials Science Center, Report No. 2839.

[1]H. Hasegawa, Prog. Theor. Phys. 21, 483 (1959).
[2]P. Monod and S. Schultz, Phys. Rev. 173, 645 (1968).
[3]S. Schultz, M. R. Shanabarger, and P. M. Platzman, Phys. Rev. Lett. 19, 749 (1967).
[4]David C. Langreth and John W. Wilkins, Phys. Rev. B 6, 3189 (1972).
[5]John Sweer, David C. Langreth, and John W. Wilkins, Phys. Rev. B 13, 192 (1976).
[6]H. Cottet, P. Donzé, J. Dupraz, B. Giovannini, and M. Peter, Z. Angew. Phys. 24, 249 (1968).
[7]M. B. Walker, Phys. Rev. B 7, 2920 (1973).
[8]S. E. Barnes and J. Zitkova-Wilcox, Phys. Rev. B 7, 2163 (1973).
[9]S. Schultz, D. R. Fredkin, B. L. Gehman, and M. R. Shanabarger, Phys. Rev. Lett. 31, 1297 (1973).
[10]G. L. Dunifer, thesis (University of California, San Diego)

(unpublished).
[11]Y. Yafet. Arch. Sci. Geneva 27, 315 (1974).
[12]L. L. Hirst, Adv. Phys. 21, 759 (1972).
[13]D. Davidov, C. Rettori, R. Orbach, A. Dixon, and E. P. Chock, Phys. Rev. B 11, 3546 (1975).
[14]J. H. Pifer and R. T. Longo, Phys. Rev. B 4, 3797 (1971).
[15]S. E. Barnes, J. Dupraz, and R. Orbach, J. Appl. Phys. 42, 1659 (1971); 42, E5908 (1971).
[16]L. L. Hirst, Phys. Kondens. Mater. 11, 255 (1970).
[17]L. L. Hirst, Z. Phys. 244, 230 (1971).
[18]L. L. Hirst, Z. Phys. 241, 9 (1971).
[19]See B. Caroli, P. Lederer, and D. Saint-James, Phys. Rev. Lett. 23, 700 (1969), and references therein.
[20]E. Ditlefsen and J. Lothe, Philos. Mag. 14, 759 (1966).
[21]M. D. Daybell and W. A. Steyert, Phys. Rev. Lett. 18, 398 (1968).
[22]W. M. Star and G. J. Nieuwenhuys, Phys. Lett. A 30, 22 (1969).
[23]W. M. Star, F. B. Basters, G. M. Nap, E. DeVroede, and C. Van Baarle, Physica (Utr.) 58, 585 (1972).
[24]Martin Albert Huisjen, thesis (Cornell University) (unpublished).
[25]J. Beuneu and P. Monod, Phys. Rev. B 13, 3424 (1976).
[26]Sheldon Schultz and Clancy Latham, Phys. Rev. Lett. 15, 148 (1965).
[27]Y. Yafet, J. Appl. Phys. 39, 853 (1968).
[28]P. Steiner, S. Hufner, and W. V. Zdrojewski, Phys. Rev. B 10, 4704 (1974).
[29]P. Monod, thesis (A. LaFaculte des Sciences D'Orsay, Universite de Paris, 1968) (unpublished).
[30]I. A. Campbell, Phys. Rev. B 10, 4036 (1974).
[31]P. Steiner and S. Hufner, Phys. Rev. B 10, 4038 (1974).
[32]M. Blume and R. E. Watson, Proc. R. Soc. Lond. 271, 565 (1963).
[33]H. Alloul, Phys. Rev. Lett. 35, 460 (1975).
[34]W. Götze, Arch. Sci. Geneva 27, 357, (1974).
[35]A. Narath, Phys. Rev. B 13, 3724 (1976).
[36]H. Alloul, J. Phys. F 4, 807 (1974).
[37]P. Steiner, W. V. Zdrojewsky, D. Gumprecht, and S. Hufner, Phys. Rev. Lett. 31, 355 (1973).
[38]D. H. McMahon, Phys. Rev. 134, A128 (1964).
[39]P. Monod (private communication).
[40]A. M. Stoneham, Rev. Mod. Phys. 41, 82 (1969).
[41]J. H. Van Vleck, *The Theory of Electric and Magnetic Susceptibilities* (Oxford U. P., London, 1972).